Future Generation Computer Systems 111 (2020) 17–26

Contents lists available at ScienceDirect

Future Generation Computer Systems

journal homepage: www.elsevier.com/locate/fgcs

Detection and diagnosis of chronic kidney disease using deep learning-based heterogeneous modified artificial neural network

Fuzhe Ma [a], Tao Sun [a], Lingyun Liu [b,*], Hongyu Jing [c]

[a] Department of Nephrology, The First Hospital of Jilin University, Changchun 130000, China
[b] Department of Andrology, The First Hospital of Jilin University, Changchun 130000, China
[c] Department of Respiratory Medicine, The First Hospital of Jilin University, Changchun 130000, China

ARTICLE INFO

Article history:
Received 4 March 2020
Received in revised form 3 April 2020
Accepted 24 April 2020
Available online 25 April 2020

Keywords:
Chronic renal failure
Kidney disease
Artificial neural network
Deep learning
Support vector machine
Segmentation

ABSTRACT

The prevalence of chronic kidney disease (CKD) increases annually in the present scenario of research. One of the sources for further therapy is the CKD prediction where the Machine learning techniques become more important in medical diagnosis due to their high accuracy classification ability. In the recent past, the accuracy of classification algorithms depends on the proper use of algorithms for feature selection to reduce the data size. In this paper, Heterogeneous Modified Artifical Neural Network (HMANN) has been proposed for the early detection, segmentation, and diagnosis of chronic renal failure on the Internet of Medical Things (IoMT) platform. Furthermore, the proposed HMANN is classified as a Support Vector Machine and Multilayer Perceptron (MLP) with a Backpropagation (BP) algorithm. The proposed algorithm works based on an ultrasound image which is denoted as a preprocessing step and the region of kidney interest is segmented in the ultrasound image. In kidney segmentation, the proposed HMANN method achieves high accuracy and significantly reducing the time to delineate the contour.

1. Introduction

Chronic Renal Disease is a leisurely loss of kidney function for months or years. Early detection of CKD is crucial and helpful in decreasing medical resources as ESRD patients preserve their health through hemodialysis, peritoneal dialysis or kidney transplantation [1]. An early detection diagnosis for CKD is commonly obtained through blood testing using the blood urea nitrogen (BUN) index and the Creatinine (CR). An analysis of patients via ultrasound images is a technical solution to do diagnosis efficiently [2]. The advantages of ultrasound imaging include various aspects such as non-invasive, radiation-free, low cost and convenience [3]. Besides, ultrasound imaging for obese patients may have less effective prediction ratio because the fat and tissue get deeper, hence its clarity becomes weaker. Ultrasonics rely primarily on the abilities of the technician in their accuracy [4]. However, the CT result offers a higher contrast picture to recognize the interior design, size, density, and structure [5]. CT images will reveal structures inside the body without overlapping structures where each slice of the 2D CT scan reveals the stone shape as shown in Fig. 1(a) and (b).

In recent years work in medical imaging has concentrated on the segmentation of kidney stones and renal cavity [6]. Candidates are freed from the pressure of manual marking by automated segmentation with potential clinical medicine, whereas only quantitative analysis enables precisely to diagnose and model kidney disease [7]. This is not a common clinical practice; however, the segmentation of automatic stones is the segmentation of automatic renal stone remains a well-studied research topic [8]. Automatic stones segmentation is mainly due to the renal stone shape, color, texture, and location of anatomical structures. Based on the stone, Kidney diseases are typically classified as hereditary, congenital, or acquired. Calcification detection within the body is a wide range of study including several diverse areas that are mainly useful for the diagnosis of kidney stone diseases [9,10].

The actual kidney stones approximately non-sphérical, although they are dependent on the reverberation time over their duration, the main effect is used to detect a fracture of actual kidney stones [11]. The segmentation of stones from such images is very complex and challenging because powerful speckle and attenuated artifacts occur in abdominal ultrasound pictures [12]. This role is therefore performed using a great deal of previous information such as texture, shape, organ spatial location, etc [13]. In this paper, the Internet of Medical Things (IoMT) has been utilized and the IoMT platform makes seamless, autonomous data collection and integration, saving time and cost for health care

* Corresponding author.
E-mail address: tmxlly@jlu.edu.cn (L. Liu).

https://doi.org/10.1016/j.future.2020.04.036
0167-739X/

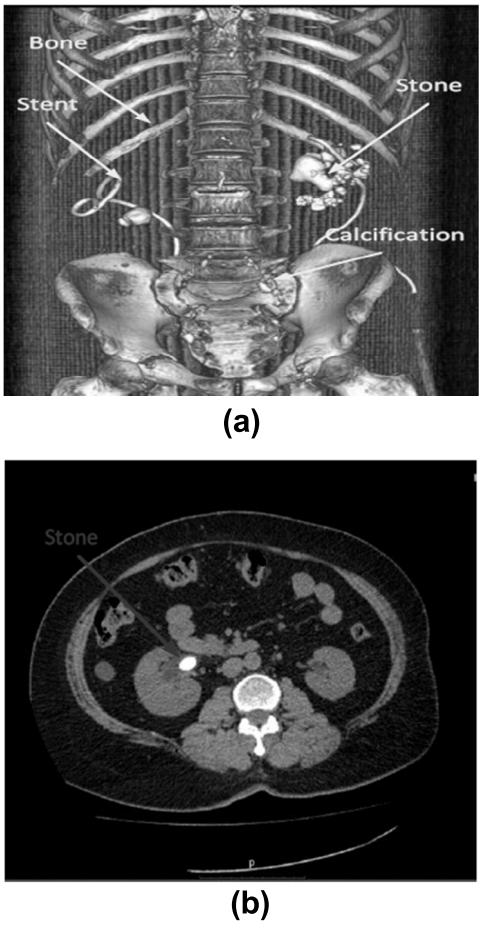

Fig. 1. (a) Stent, Stone, Calcification and bone on CT Image (b) CT Slice.

providers. The most widely used tool for the treatment of disease is the Artificial Neural Network (ANN) [14–17] in the present scenario of medical diagnosis research. Due to defect tolerance, generalization, and environmental learning capabilities of artificial neural networks, medical diagnosis fields are becoming more common [18]. The feed-forward network, which permits network connection only between nodes on one layer and those on the next layer, is one of the commonly used network architectures. Neural network feedback is used to differentiate between infected individuals as a classifier [19,20].

The main contributions of the paper as follows:

- The deep learning-based Heterogeneous modified artificial neural network (HMANN) has been proposed to predict and diagnosis Chronic kidney disease (CKD).
- Developing algorithms to derive meaningful semantic from digital images constitutes in computer vision and machine learning.
- An experienced radiologist has been checked to separate MR as well as CT scan images of the abdominal into the left and right portion to produce the reference standard for segmentation from the validation and training datasets.

The remainder of the paper is organized as follows: Sections 1 and 2 discussed the background of Chronic kidney disease and existing methods. Section 3 discussed the problem description and machine learning algorithm to define and segment the kidney disease. In Section 4, the experimental results have discussed. Finally, Section 5 concludes the research article.

2. Related works

Shi Yin et al. [21] proposed the Subsequent Boundary Distance and Pixelwise Classification networks (SBD-PCN) for automatic ultrasound image kidney segmentation. First, Authors reported pre-trained deep neural networks to classify images for high-level images from Ultrasound (US) images, then used these functions as input for the learning of kidney boundaries maps with an intermediate distance regression network and finally they classify the recognized boundary distance maps into kidney pixels with a network of pixel classification. The segmentation of the kidney image is based on deep CNNs to predict kidney and kidney borders in a final learning way.

Jamshid Norouzi et al. [22] introduced the Adaptive Neuro-fuzzy Inference System (ANFIS) to predict chronic renal failure. Here, the number of fuzzy rules corresponds to the number of input variables ' membership functions. ANFIS neural networks had been used for the identification of glomerular filtration rates and comparison of system accuracy. Modeling and prediction results from ANFIS networks demonstrate the models based on the fuzzy method to estimate extremely accurate GFR. The efficacy and regular monitoring of CKD patients in reducing disease progression and preventing the inevitable complications are major concerns of clinicians. An important method for increasing its burden in using the efficient prediction model initialized this study for decision support in the area of kidney disease and CKD management in a statistical manner.

JIANXIN CHEN et al. [23] initialized the Pattern Discovery Algorithm based on the delineated revised mutual information (PDA-ADMI) in chronic kidney failure. A revised version of mutual information to distinguish the negative and positive associations is provided in this paper. The authors discovered 16 effective patterns about the syndrome which were manually verified by physicians. They proved that the cluster is superadditive by shared information and incorporated n-class association principles into the PDA-ADMI model to decrease the complexity of computation. Algorithm testing was carried out using syndrome data and medically compiled to consist of 16 patterns.

Vijaya B. Kolachalama et al. [24] introduced the Pathological estimated Fibrosis score (PEFS) based on deep learning for the detection of chronic renal disease. They utilized a deep learning technique to merge patient-specific histological objects with clinical phenotypes, such as serum creatinine, nephrotic proteinuria at biopsy, chronic kidney disease (CKD), renal survival for 1 to 3, and 5 years. The proposed CNN models exceeded PEFS during classification tasks and detect the stage for the CKD more accurately than the system PEFS.

Njoud Abdullah Almansour et al. [25] proposed the Artifical Neural Network and Support vector machine (ANN-SVM) for the prediction of chronic kidney disease. All missing data values have been replaced by the mean of the respective attributes for experiments to be carried out. Afterward, the optimal parameters are calculated by Artificial Neural Network (ANN) and Support Vector Machines (SVM) based on numerical analysis. Further, the Optimized parameters were identified for the Support Vector and Artificial Neural Network.

To overcome various issues as discussed in the above survey, our investigation deals with the HMANN approach which has been proposed for the kidney stone recognition process. Further, wavelets and ANN for clinical classification results indicate the highest accuracy. In addition, when partial diseases are identified and observed the diagnosing disease can be beneficial if time and data are limited. This paper utilizes Artificial neural networks to provide an excellent method for a partial diagnosis.

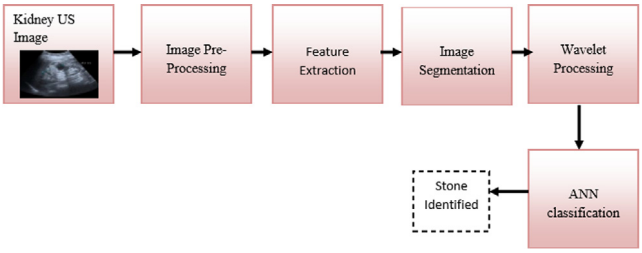

Fig. 2. The Proposed HMANN Block Diagram.

3. Problem description

The malfunction of the kidneys can threaten life, so it is crucial to detect kidney stones early. It is necessary to locate the site of the kidney to perform surgery for removing a kidney stone. The ultrasound kidney images are of low contrast and consist of speckles, making it difficult to distinguish kidney anomalies. This may make it difficult for doctors to correctly identify small kidney type and stones. To address this issue, the proposed sub-bands of wavelets have been used to extract energy levels of stone and the HMANN classification algorithms of SVM and MLP-BP.

3.1. Heterogeneous Modified Artificial Neural Network (HMANN)

In this paper, a deep learning-based Heterogeneous Modified Artifical Neural Network (HMANN) method has been proposed for the early detection, segmentation, and diagnosis of chronic renal disease. In the proposed HMANN system, the noise must be reduced after acquiring a raw image, as it can be an important segmentation problem. The pre-treatment technique based on a wavelet is used to minimize noise. The denoted image segments the kidney area and extracts more processing features of characteristics that have been chosen to indicate an abnormality in the kidney. Fig. 2 shows the proposed HMANN block diagram and workflow.

3.1.1. Pre-processing

The received image of the US contains low contrast noise which can lead to a failure to assess image quality. The location of the kidney stone is very critical for surgery. Pre-processing of the ultrasound image is necessary to conquer low contrast and speckling noise. In the case of an abnormal stage, a classifier for SVM is used to predict kidney stones or cysts. The priority of sending patient data can be modified in the event of an emergency depending on the classification decision. The kidney is labeled with a circle in both normal and abnormal cases of cysts and stones. Speckle noise reduction is an activity that improves ultrasound quality by retaining image characteristics. Reducing the noise in the image would enhance the organ contour and make it easier to segment the US images. Specks have been denoised using threshold wavelet coefficients because in the wavelet domain image nature is small. The pre-processing kidney image contains three stages. (i) Restoration of Image, (ii) Sharpening and Smoothening, and (iii) Contrast Enhancement. Fig. 3 explains the pre-processing system.

3.1.2. Restoration of image

The aim of image restore is precisely processed to reduce the damage done by the US scan acquisition. The level set method is used in this system for the correct orientation. Throughway of curve motion, shrinks are gradually removed by the application of curve motion.

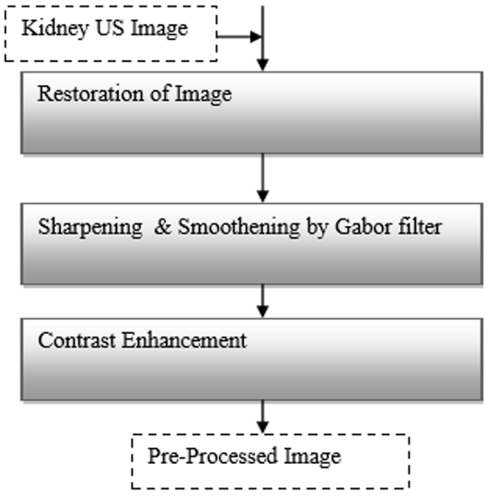

Fig. 3. Image Preprocessing.

3.1.3. Sharpening and smoothening

Gabor filters serving as a bandpass filter for local spatial frequency distribution which is used to achieve optimum resolution in both frequency and spatial domains. The standard deviation from Gaussian will differ to change the smoothness degree. The original image and denoised image are shown in Fig. 4(a) and 4.(b) which are taken from the datasets (https://archive.ics.uci.edu/ml/datasets/Chronic_Kidney_Disease) respectively.

3.1.4. Contrast enhancement

The histogram equalization is employed to enhance contrast and achieve uniform intensity. This technique can be used on an entire image or part of an image. The contrast of the images has been improved in this method by converting the values to an intensity object of the histogram output image matches for approximation. The output value is similar to the input value.

3.2. Image segmentation

Due to the massive nonrigid existence of the kidney, manually separated areas of interest from kidney ultrasound images by scanning artifacts such as acoustic shadows, low signal to noise ratios and low contrast have been validated. A graphical user interface is developed for manual segmentation to extract the region of kidney interest. In this paper, marked points along the outline of the renal and cubic spinal interpolation between the spots to achieve a smooth outline has been shown in Fig. 5(a), (b), (c), and (d) on CKD detection and segmentation from CT acquisitions of different patients.

In the context of image processing, the primary purpose of saliency detection is to distinguish between relevant and non-relevant pixels in a given set of images. Therefore, this definition is specific and closely related to the desired application of kidney stone segmentation. A variational detection model for saliency has been introduced and mathematically expressed for the saliency detection in kidney stone segmentation.

$$\min_{v \in AU(\Omega) \bigcap [0,1]} I(v) + \frac{1}{\beta^2} G(v) + \frac{\lambda}{\beta} H(v) \tag{1}$$

As shown in Eq. (1) where $\Omega \subset \mathbb{R}^c, c = 2, 3$ is the image domain, I(v) is the Functional regularization, $G(v)$ is the concave definition of energy modeling saliency, Further, $H(v)$ defines the fidelity to restore records of λ and β variable which denote the positive real values. Assuming that having only Gaussian noise

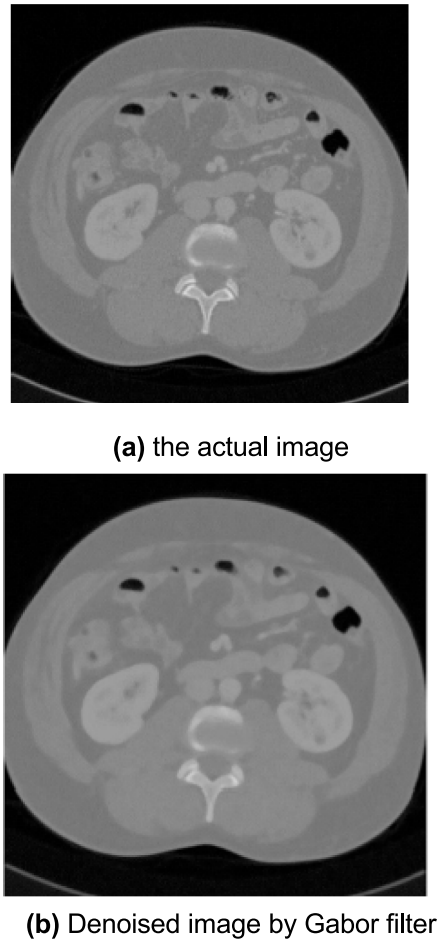

Fig. 4. Image analysis using filter.

and no other corrupting effect has been mathematically shown in the Eq. (2),

$$H(v) = \frac{1}{2}\int_{\Omega}(v-f)^2 \tag{2}$$

As shown in Eq. (2) where $f(y) \in K^{\infty}(\Omega)\bigcap[0,1]$ is given data which is substituted to get the saliency term G(v) expressed as in Eq. (3),

$$H(v) = \int_{\Omega} g(v)dy = -\frac{1}{2}\int_{\Omega}(1-\alpha v)^2 \tag{3}$$

As shown in Eq. (3) where α is a positive real variable. The term G(v) promotes detection by regions with no relevant information (background) of salient regions of interest (foreground). Note that if no term of diffusion or fidelity is considered, the term of saliency would act as a simple, non-homogeneous threshold. The salient term solves the problem of segmentation and reduces complexity.

3.3. Feature extraction

Manual segmentation takes place in the presence of a well-trained doctor on normal and abnormal images. The features required for kidney characterization which are derived from segmented areas. These can be classified into 3 classes: Haralick features, Histogram features, and adaptive features. Many features include the size, position, and texture of the echo. The term adaptive indicates various traits between individuals and

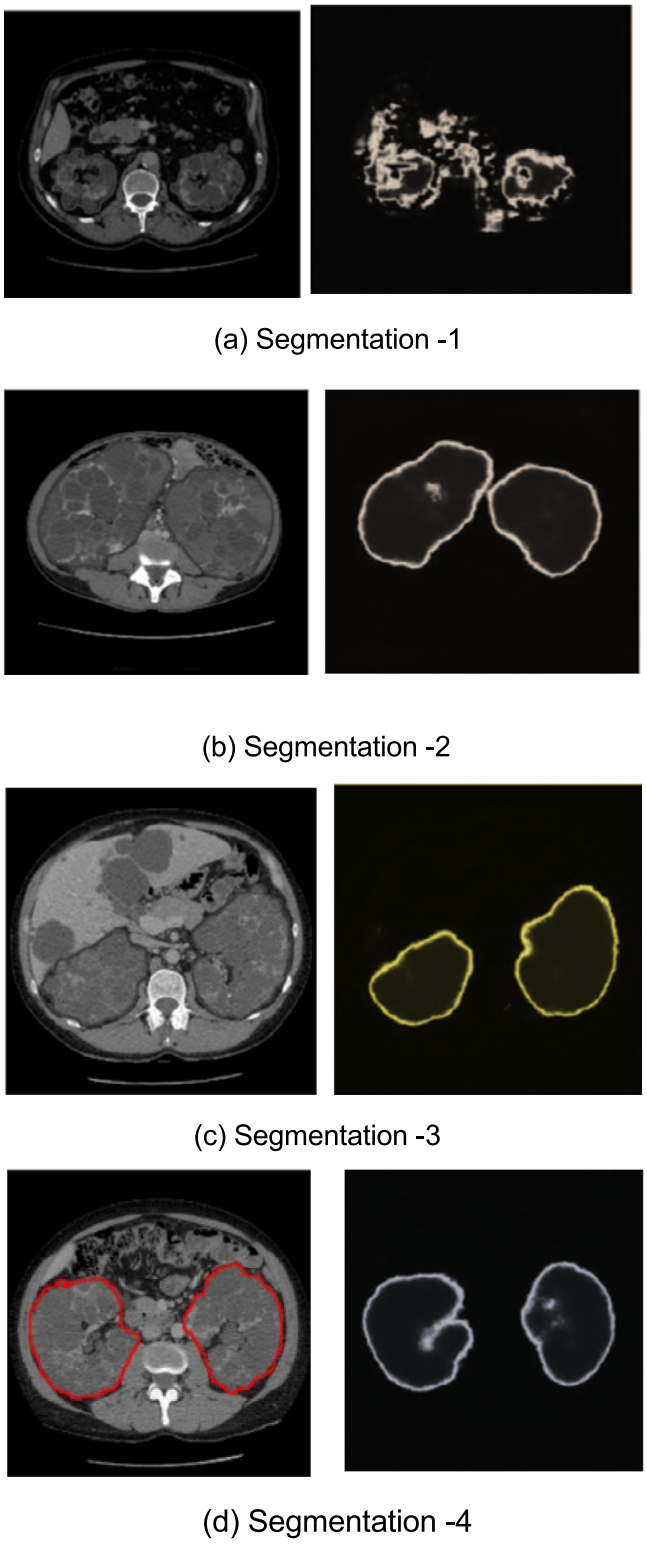

Fig. 5. (a–d). Four Segmentation of Chronic Kidney Disease (CKD) from CT acquisition of different Patients taken from (https://archive.ics.uci.edu/ml/datasets/Chronic_Kidney_Disease).

cannot be generalized. The histogram derived extract offers statistical features of a first-order object, which are useful for organ preservation and classification. Furthermore, features are analyzed using gray-level co-occurrence matrix (GLCM) that includes

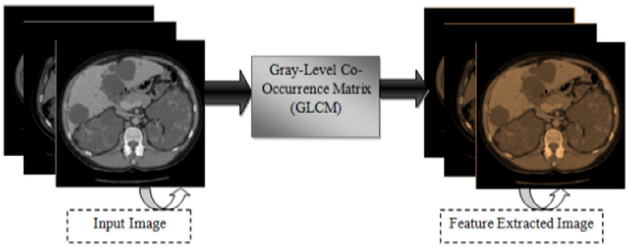

Fig. 6. Feature extraction process using GLCM.

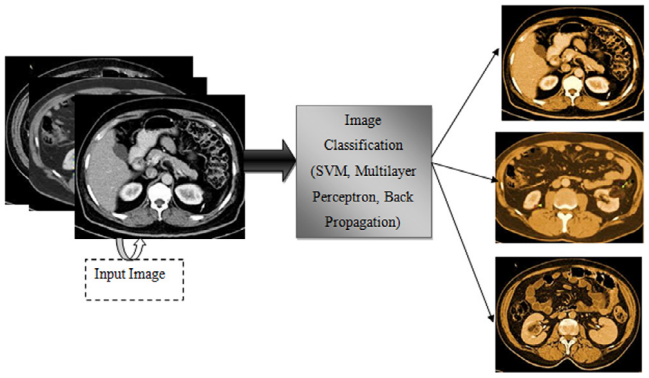

Fig. 7. Image Classification process.

contrast, correlation, autocorrelation, prominence in the clusters, the shade of the cluster, homogeneity, dissimilarity, high likelihood, average amount, square sum, sum variance, variance, total entropy, differential entropy, correlation measurement, and inverse. Fig. 6 shows the Feature extraction process using GLCM functions.

These are extracted from the H of dimension M_h co-occurrence matrix (gray level number), each of the Q(j, i) elements gives the probability of gray level j occurrence in the defined spatial relationship with gray level I with various mathematical computation as formulated as follows,

$$H = \begin{bmatrix} Q(1,1) & \dots & Q(1,M_h) \\ \vdots & \ddots & \vdots \\ Q(M_h,1) & \dots & Q(M_h,M_h) \end{bmatrix} \tag{4}$$

$$\mu_y = \sum_{j=1}^{M_h} jQ_y(j) \tag{5}$$

$$\mu_x = \sum_{i=1}^{M_h} iQ_x(i) \tag{6}$$

$$\sigma_y^2 = \sum_{j=1}^{M_h} (Q_y(j) - \mu_y)^2 \tag{7}$$

$$\sigma_x^2 = \sum_{i=1}^{M_h} (Q_x(i) - \mu_x)^2 \tag{8}$$

$$Q_y(j) = \sum_{j=1}^{M_h} Q(j,i) \tag{9}$$

$$Q_x(j) = \sum_{i=1}^{M_h} Q(j,i) \tag{10}$$

$$Q_{y+x}(l) = \sum_{j,i=1}^{M_h} Q(j,i) \tag{11}$$

As shown in the above equations where σ_y, $\sigma_x\mu_y$, μ_x, are the standard deviation and mean of Q_y and Q_x. $Q_y(j)$, $Q_x(i)$ is the sum of the jth row and ith column correspondingly.

3.4. Feature selection

Histogram functions give a distribution of the intensity of an image including kurtosis, mean, skewness, entropy and variance. From this kurtosis and mean, skewness has been selected from histograms and the cluster shade feature is picked from Haralick features, based on standard deviation from every metric for images which are measured individually, to improve the trained classifier parameter size. There is the least variance in the homogeneity has found with high probability, correlation, average sum, and square sum compared to other features. In addition to taking all the features into account, these 9 streamlined features are considered for further classification. The following parameters are determined for these features,

$$\max prob = \sum_{j,i=1}^{M_h} \max(Q(j,i)) \tag{12}$$

$$mean,\ \mu = \frac{1}{NM} \sum_{j,i} J(j,i) \tag{13}$$

$$skewness = \frac{1}{NM} \sum_{j,i} \frac{(J(j,i) - \mu)^3}{\sigma^3} \tag{14}$$

$$Kurtosis = \frac{1}{NM} \sum_{j,i} \frac{(J(j,i) - \mu)^4}{\sigma^4} \tag{15}$$

$$cluster\ shade = \sum_{j,i} \left(j + i - \mu_y - \mu_x\right)^3 Q(j,i) \tag{16}$$

$$homogeneity = \sum_{j,i} \frac{Q(j,i)}{1 + |j - i|} \tag{17}$$

$$sum\ avg = \sum_{j,i=1}^{2M_h} \frac{\{j \times i\} \times Q(j,i) - \{\mu_y \times \mu_x\}}{\sigma_y \sigma_x} \tag{18}$$

$$sum\ of\ squares = \sum_{j,i} \left(j - \mu_y\right)^2 Q(j,i) \tag{19}$$

3.5. Classification

The proposed HMANN method classification divided into three architectures is namely, Support Vector Machine (SVM), Multilayer Perceptron and Back Propagation algorithms. Fig. 7 shows the image classification process using Support Vector Machine (SVM), Multilayer Perceptron, Back Propagation.

3.5.1. Support Vector Machine (SVM)

Support vector machines (SVM) are a set of supervised learning approaches utilized to identify, regress, and detect outliers. SVM methods are designed using learning algorithms to support data analysis and pattern recognition which are mathematically expressed in the algorithm.1. as follows,

Algorithm 1: Kidney Stone Classification

Input: Dataset $E = \{(y_1, x_1), (y_2, x_2), \ldots .(y_n, x_n)\}$
Number of learning rounds R
Base learning algorithm $\mathfrak{L}$
Process:
$E_1(j) = 1/n$ #Introduce the weight distribution
For r=1,...R
$g_r = \mathfrak{L}(E, E_r)$; #Train a Learner gr from E using distribution E_r
$\varepsilon_r = Qt_{y\sim E_r,x} J[g_r(y) \neq x]$; #Error Measure of g_r
If $\varepsilon_r > 0.5$ then break
$\beta_r = \frac{1}{2}\ln\left(\frac{1-\varepsilon_r}{\varepsilon_r}\right)$; #identify the weight of g_r
$E_{r+1}(j) = \frac{E_r(j)}{Z_r}\begin{cases}\exp(-\beta_r)\, if g_r(y_j) = x_j \\ \exp(\beta_r)\, if g_r(y_j) \neq x_j\end{cases} = \frac{E_r(j)\exp(\beta_r x_j g_r(y_j))}{Z_r}$
#Update the distribution where Normalization denoted by Z_r which enables E_{r+1} to be distribution
End
Output:
$G(y) = sign(\sum_{r=1}^{R} \beta_r g_r(y))$

If classification in a high-size feature space is easier, to create in this space a maximum margin hyperplane has been selected to optimize the distance between hyper-plane and closer support vectors on both sides. The design relies on internal products, in the feature space. If the dimensions become too large, this can be computationally unstable. At the training, SVM is trying to create a model that better defines the features of two various classes. SVM utilizes an optimization approach to define the W_j, weights S_j and Bias A vectors which are used to classify Y vectors as follows:

$$X = \sum_j S_j L\left(W_j, Y\right) + A \tag{20}$$

As shown in Eq. (17), where L is the Kernel Function. SVM classifier uses different kernel functions such as radial, polynomial, linear, multilayer perceptron. L is the point product for a linear kernel. If X is high, then Y is categorized as part of the first group, otherwise, it has been categorized as part of that second group. In the SVM classifier, the various kernels used are:

a. Linear SVM:

If C is the normal and abnormal image training data with several m images, the format can be shown,

$$C = \left(\left(y_j, x_j\right) \middle| y_j \in T^q, x_j \in (-1, 1)\right)_{j=1}^{m} \tag{21}$$

As shown in Eq. (18) where x_j is 1 or -1, denoting the class to which y_j belongs.y_j is a two-dimensional matrix, y_1 is the normal image dataset and y_2 is the abnormal image dataset. Hyperplane can be used in the linear kernel to distinguish objects with $x_j = 1$ and $x_j = -1$.

b. Polynomial Kernel

The polynomial Kernel is stated as follows,

$$l(y, x) = (y^R x + b)^c \tag{22}$$

As shown in Eq. (19) where y and x are vectors in the input space. Feature vectors evaluated from test and training samples where c is set to 3 and b is set to 0 which are calculated for the homogeneous kernel with backpropagation model as defined in the algorithm.2.

Algorithm:2. Multilayer Perceptron — Back Propagation Algorithm

Input: j,i, l
Output: y,x
For (i=1)
$X = \sum_j S_j L\left(W_j, Y\right) + A$For (j=0)
$C = \left(\left(y_j, x_j\right) \middle| y_j \in T^q, x_j \in (-1, 1)\right)_{j=1}^{m}$If (j > i)
$l(y, x) = (y^R x + b)^c$else
$l(y, x) > (y^R x + b)^c$End for
End for
End if
End
Return

c. Radial basis function kernel

The Gaussian kernel is a radial function kernel which has two y and y' samples, representing vectors for the given image. The definition is:

$$l\left(y, y'\right) = \exp\left(\frac{\left\|y - y'\right\|^2}{2\sigma^2}\right) \tag{23}$$

As shown in Eq. (20) where $\left\|y - y'\right\|^2$ is the Euclidean distance squared between vectors of features. σ is the Gaussian Kernel variance and is set to 1.

3.5.2. Multilayer perceptron

Multilayer Perceptron is analogous to a neural network and known as a tangent kernel hyperbolic. It blends several perceptions on a single layer. The sigmoid shaped transfer function, like tangent hyperbolic or logistic function, which is used by every single layer perceptron as expressed as follows,

$$l\left(y, y'\right) = \tanh(\rho\left(y, y'\right), \beta) \tag{24}$$

In the proposed deep learning-based Heterogeneous Modified Artificial Neural Network (HMANN) for detecting, segmentation, and diagnosis of chronic kidney disease. SVM has been utilized to classify the presence of cyst or stone in the kidney with a multilayer perceptron (MLP) classifier with extracted features. The proposed method reduces the noise of ultrasound images and enhances the image quality using level set segmentation.

Machine learning algorithms are either used as normal or abnormal for the classification of kidney images. The main goal of ML algorithms is to learn and draw intelligent conclusions automatically. The weak classifier may be generated in the classification process which may diminish the classifier's accuracy. In this method, by increasing the weights, the misclassified samples are fixed. As a result, using the supervised learning algorithm, the strong classifier has been developed.

The artificial neural network algorithm feeds forward with a multi-layer perceptron mapping energy values from the extraction of sub-band wavelets. Such energy values are supplied with the input layer and multiplied with the backpropagation process for a non-linear activation process which is performed by three or more hidden layers. The back-up is the most used multi-layer learning algorithm in the neural system which uses gradient descent to reduce the squared error from the output value of the network to the desired output level. Such error signals are utilized to measure the energy updates of the data acquired by the network. The main algorithms are Multilayer Back Propagation Perceptron (MLP-BP). The accuracy, speed, and performance of the proposed MLP-BP algorithm are better than others. As the Data can be further analyzed from these devices to produce future forecasts. The IoMT or Healthcare IoT has been used which has a range of internet-enabled medical devices

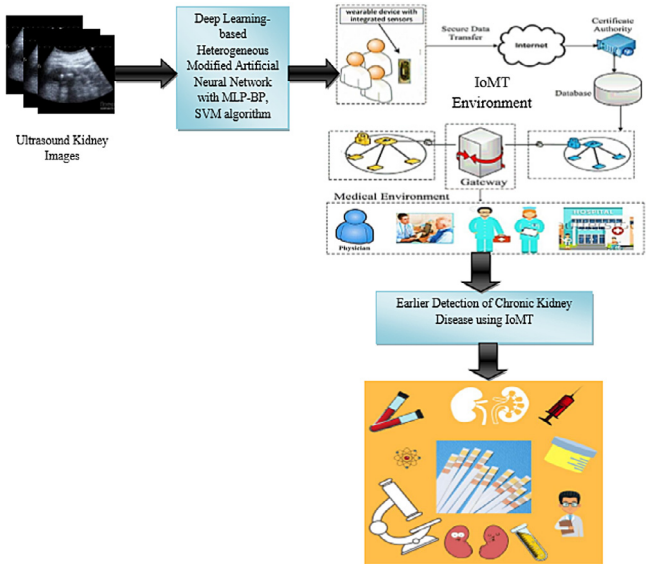

Fig. 8. Chronic Kidney Disease Detection using deep learning on IoMT Platform.

Table 1
Overall classification accuracy.

Number of Datasets	SBD-PCN	ANFIS	PDA-ADMI	PEFS	ANN-SVM	HMANN
10	33.5	35.1	36.8	39.3	41.3	51.6
20	40.3	43.5	48.9	60.3	63.4	69.2
30	55.2	56.8	59.2	60.8	69.3	78.2
40	68.2	77.4	81.3	85.6	87.2	89.9
50	78.3	88.9	89.2	91.7	92.3	97.5

and applications that interconnect independently (machine-to-machine communications) with a cloud platform like AWS. The IoMT can even be used for tracking information from ICU, ECG, abnormalities in kidney detection, treatment of conditions such as cancer, and many more sensory devices including implantable pills heartbeat sensors, or IoMT. Fig. 8 shows the Chronic Kidney Disease Detection using Deep Learning on the Internet of Medical Things Platform.

4. Experimental results

4.1. Overall classification accuracy

In this paper, the suggested HMANN method with a comparison of the overall classification accuracy according to the scale of the different methods, to understand the learning dependency of the different techniques. The proposed method achieves high accuracy in predicting kidney stones when compared to other existing methods. Fig. 9(a) shows the overall accuracy of the proposed HMANN method. Fig. 9(b) shows the dice accuracy. All patients in training are pre-treated using the ANN methodology. Using 640 teaching subjects, network training has been allowed to run for 300 epochs. Achieve 0.98 dice accuracy with training data and 0.93 with a subset of patients with improved training.

A comprehensive and accurate diagnosis of kidney cancer is the first step in developing a plan for treating kidney cancer. Fig. 10(a) shows the CT scan and the accuracy of predicting the stone in the right lower lobe module. Fig. 10(b) shows the left kidney CT scan with metastasis.

Table 1 shows the overall classification accuracy of the proposed HMANN approach. Different kernels are used with an SVM classifier, which has been used to identify abnormal images according to a kernel with a multilayer perceptron accuracy of

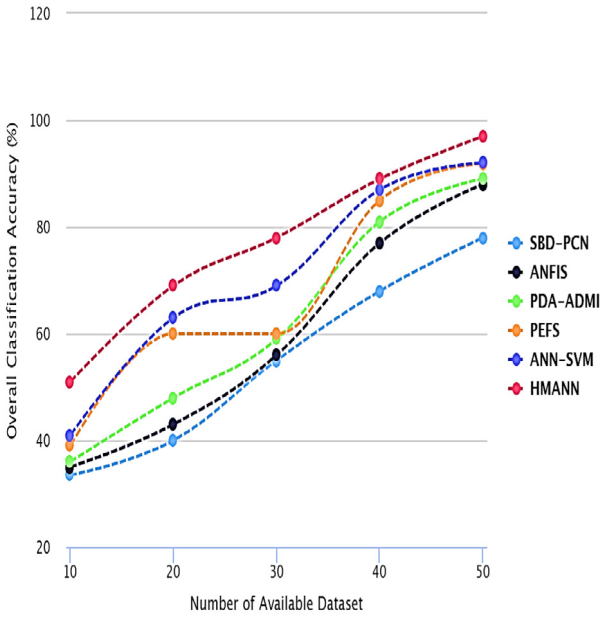

(a) Overall Classification accuracy

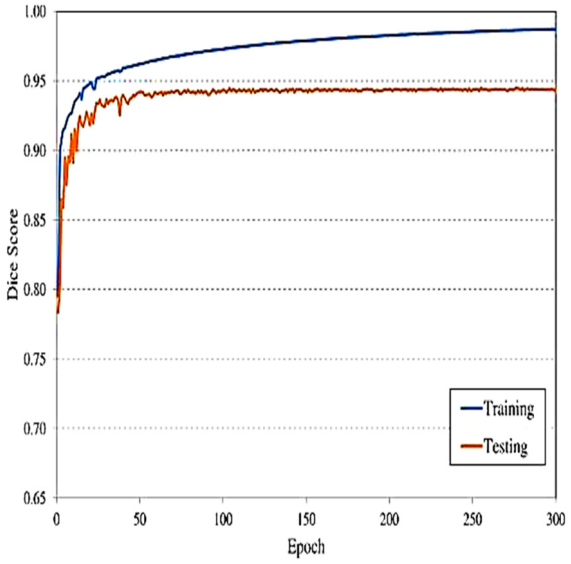

(b) Dice Accuracy

Fig. 9. Accuracy analysis.

97.50% percent. However, the availability of this data helps recommend immediate prevention and monitoring of disease progression.

4.2. Overall classification accuracy

The performance of the proposed segmentation has been analyzed with various images and described in Section 3. The SVM classification is tested with polynomial, Radial, linear, MLP and Basis Function (RBF) kernels to evaluate the performance in the SVM kernel to classifying the abnormality. In the experimental analyses section, the performance of every kernel is recorded, and the MLP kernel performed better in the classification of abnormal kidney images compared to other kernels. The proposed HMANN method achieves a high-Performance ratio when compared to other SBD-PCN, ANFIS, PDA-ADMI, and ANN-SVM

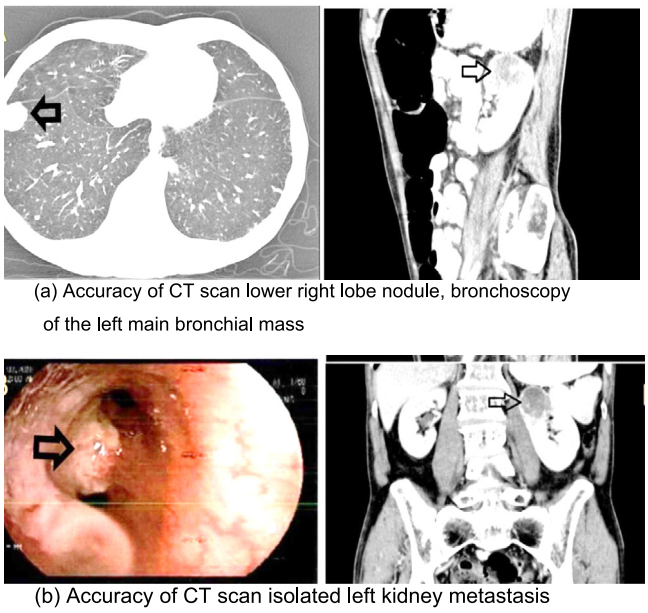

Fig. 10. CT Scan image for kidney metastasis.

Table 2
Prediction ratio.

Available Datasets	SBD-PCN	ANFIS	PDA-ADMI	PEFS	ANN-SVM	HMANN
10	78.1	79.4	80.4	81.2	82.9	87.3
20	65.3	68.3	69.8	70.2	72.3	74.1
30	55.2	56.8	59.2	67.2	68.1	79.5
40	80.3	87.6	89.3	90.2	91.3	92.7
50	68.8	79.4	89.2	94.7	96.1	99.7

methods. Fig. 11(a) demonstrates the performance ratio of the proposed system. Fig. 11(b) shows the overall survival rate of the patients after diagnosis. The progression rate is based on age, underlying diagnosis, secondary preventive measures and effectiveness of the individual patient. The early start of chronic renal substitution treatment is essential if uremic CKD complications can lead to major disease and death. It is important to prevent these complications.

4.3. Prediction ratio

Classification is equivalent to clustering because it also collects information in segments called classes The algorithm uses a training set with a set of attributes and the corresponding result, which are commonly called the target or prediction attribute, to predict the outcome. The appropriate selection parameters for the tests of different kernels show interpreted results to develop better prediction learning techniques. The proposed HMANN method has a high prediction ratio when compared to other existing methods. Fig. 12(a) Prediction ratio of the proposed system. Fig. 12(b) shows the AUC curve of Sensitivity and Specificity. The feature for the learning model for the machine has been completely derived and contributed to the unprecedentedly high accuracy of prediction. The qualitative analysis of autosomal dominant polycystic kidney disease candidates has been validated in this model.

Table 2 shows the prediction ratio of the proposed HMANN method. SVM and MLP-BP algorithm can be used for prediction along with classification. The classification matrix shows the correct and incorrect predictions rate. The values in the test dataset are correlated with the values in the trained model.

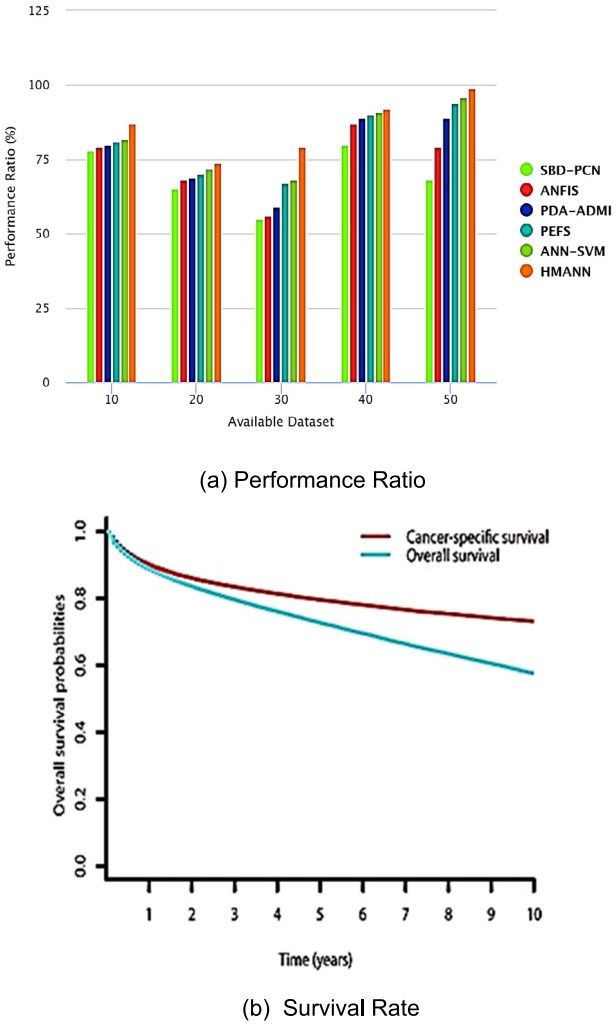

Fig. 11. Performance ratio Vs Survival rate.

4.4. Computational time

The performance is validated by the error and computation time of the selected classifier. Sensitivity and specificity are predicted for classification accuracy. The time of computation is considered for each classifier. The proposed HMANN system achieves low computation time for high sensitivity, specificities, and accuracy. The segmented stone area uses traditional segmentation algorithms by the segmentation process. Fig. 13. demonstrates the computational time of the proposed HMANN system.

4.5. Receiver Operating Characteristic (ROC)/Area Under Curve (AUC)

The ROC curve shows the output visually while the AUC clearly shows the quantitative metric. Finitely many points are made of the image of the ROC curve. It is traditional to interpolate linearly under the dictionary order when plotting the curve of ROC between neighboring points. A successful classifier's ROC curve will have a steep positive path close to its source and will reach the square unit ceiling rapidly. The ROC curve of a poor category is gentler and closer to the line. The area of the AUC is bounded by the bottom of the square and the ROC curve. Closer to 1 AUC scoring is a good performance, whereas a closer AUC

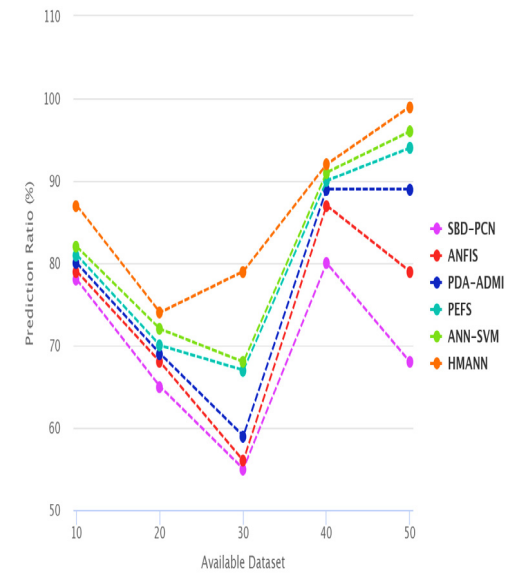

(a) Prediction Ratio

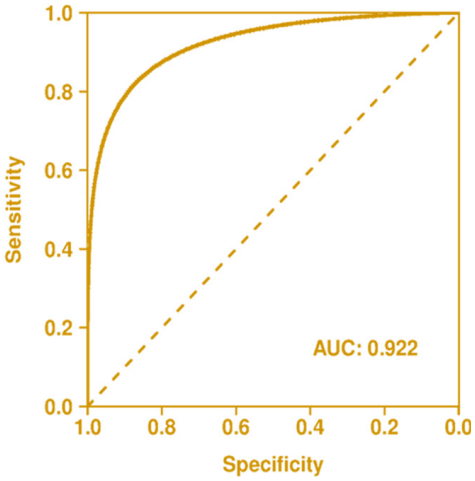

(b) Sensitivity and Specificity AUC

Fig. 12. Prediction Vs Sensitivity and Specificity AUC analyses.

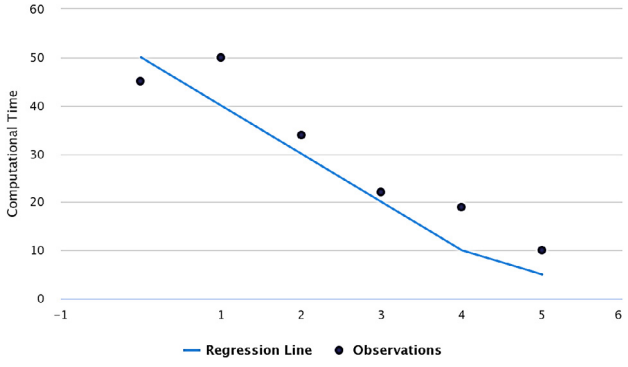

Fig. 13. Computational Time.

is 0.50 indicating poor performance. Fig. 14 shows the ROC/ AUC curve of the proposed HMANN method.

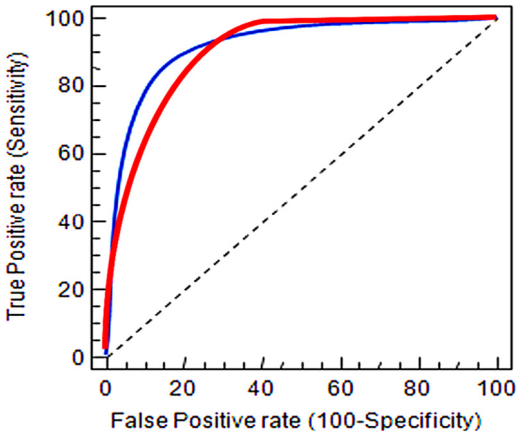

Fig. 14. Receiver Operating Characteristic Curve.

The concepts developed in this study were used and tested using data gathered at dialysis sites. The results of the computation were reported Eventually, HMANN is recommended for renal dialysis to achieve improved accuracy and performance tests. The experimental results show high accuracy, performance for detecting the early detection and diagnosis of Chronic renal failure.

5. Conclusion

This paper presents a deep learning-based Heterogeneous Modified Artifical Neural Network (HMANN) method for the detection of chronic renal disease. There are some noisy and complexity during image segmentation. Therefore, it needs an algorithm to manage missing and noisy values with a classification capability. The Proposed HMANN method reduces the noise and helps to segment the kidney image for the clear identification of kidney stone location. To find a good solution to this problem tested three classifiers: support vector machine, artificial neural networks, and Multilayer perceptron. In this paper, the performed feature reduction with the help of significant results from this study, both to reduce excess fitness and to identify the most significant predictive attributes for CKD. Besides, the new factors have found that classifiers use for more accurate detection of CKD than modern formulation.'

Declaration of competing interest

The authors declare that they have no known competing financial interests or personal relationships that could have appeared to influence the work reported in this paper.

CRediT authorship contribution statement

Each individual has made an outstanding contribution to the research for this study. Fuzhe Ma and Yujing Hong designed the research framework and algorithm and wrote the manuscript, also equally contributed to this work. Tao Sun improved and optimized the entire algorithm, and Lingyun Liu was responsible for revising and checking the manuscript.

Acknowledgments

Fuzhe Ma and Hongyu Jing designed the research framework and wrote the manuscript, and they equally contribute to this work.

References

[1] Anusorn Charleonnan, et al., Predictive analytics for chronic kidney disease using machine learning techniques, in: 2016 Management and Innovation Technology International Conference, MITicon, IEEE, 2016, http://dx.doi.org/10.1109/MITICON.2016.8025242.

[2] Navdeep Tangri, et al., A predictive model for progression of chronic kidney disease to kidney failure, JAMA 305 (15) (2011) 1553–1559.

[3] Abdulhamit Subasi, Emina Alickovic, Jasmin Kevric, Diagnosis of chronic kidney disease by using random forest, in: CMBEBIH 2017, Springer, Singapore, 2017, pp. 589–594.

[4] Asif Salekin, John Stankovic, Detection of chronic kidney disease and selecting important predictive attributes, in: 2016 IEEE International Conference on Healthcare Informatics, ICHI, IEEE, 2016, http://dx.doi.org/10.1109/ICHI.2016.36.

[5] Michael G. Shlipak, et al., Cardiovascular mortality risk in chronic kidney disease: comparison of traditional and novel risk factors, JAMA 293 (14) (2005) 1737–1745.

[6] Zeid Khitan, et al., Predicting adverse outcomes in chronic kidney disease using machine learning methods: data from the modification of diet in renal disease, Marshall J. Med. 3 (4) (2017) 68–80.

[7] Josef Coresh, et al., Prevalence of chronic kidney disease in the United States, JAMA 298 (17) (2007) 2038–2047.

[8] Tamara Isakova, et al., Fibroblast growth factor 23 and risks of mortality and end-stage renal disease in patients with chronic kidney disease, JAMA 305 (23) (2011) 2432–2439.

[9] Nisha I. Parikh, et al., Cardiovascular disease risk factors in chronic kidney disease: overall burden and rates of treatment and control, Arch. Intern. Med. 166 (17) (2006) 1884–1891.

[10] Heejung Bang, et al., Screening for occult renal disease (SCORED): a simple prediction model for chronic kidney disease, Arch. Intern. Med. 167 (4) (2007) 374–381.

[11] A. Yadollahpour, Applications of expert systems in management of chronic kidney disease: a review of predicting techniques, Orient. J. Comput. Sci. Technol. 7 (2) (2014) 306–315.

[12] Jamie L. Fleet, et al., Detecting chronic kidney disease in population-based administrative databases using an algorithm of hospital encounter and physician claim code, BMC Nephrol. 14 (1) (2013) 1–8.

[13] Deepa Gupta, Sangita Khare, Ashish Aggarwal, A method to predict diagnostic codes for chronic diseases using machine learning techniques, in: 2016 International Conference on Computing, Communication and Automation, ICCCA, IEEE, 2016, http://dx.doi.org/10.1109/CCAA.2016.7813730.

[14] Rex L. Jamison, et al., Effect of homocysteine lowering on mortality and vascular disease in advanced chronic kidney disease and end-stage renal disease: a randomized controlled trial, JAMA 298 (10) (2007) 1163–1170.

[15] Alexander Arman Serpen, Diagnosis rule extraction from patient data for chronic kidney disease using machine learning, Int. J. Biomed. Clin. Eng. 5 (2) (2016) 64–72.

[16] Ayub Akbari, et al., Detection of chronic kidney disease with laboratory reporting of estimated glomerular filtration rate and an educational program, Arch. Intern. Med. 164 (16) (2004) 1788–1792.

[17] Huseyin Polat, Homay Danaei Mehr, Aydin Cetin, Diagnosis of chronic kidney disease based on support vector machine by feature selection methods, J. Med. Syst. 41 (4) (2017) 1–11.

[18] Andrew S. Levey, Lesley A. Inker, Josef Coresh, Chronic kidney disease in older people, JAMA 314 (6) (2015) 557–558.

[19] Douglas S. Keith, et al., Longitudinal follow-up and outcomes among a population with chronic kidney disease in a large managed care organization, Arch. Intern. Med. 164 (6) (2004) 659–663.

[20] S. Susan Hedayati, et al., Association between major depressive episodes in patients with chronic kidney disease and initiation of dialysis, hospitalization, or death, JAMA 303 (19) (2010) 1946–1953.

[21] Shi Yin, et al., Automatic kidney segmentation in ultrasound images using subsequent boundary distance regression and pixelwise classification networks, Med. Img. Anal. 60 (2020) 101602.

[22] Jamshid Norouzi, et al., Predicting renal failure progression in chronic kidney disease using integrated intelligent fuzzy expert system, Comput. Math. Methods Med. 2016 (2016) 1–9.

[23] Jianxin Chen, et al., An unsupervised pattern (syndrome in traditional Chinese medicine) discovery algorithm based on association delineated by revised mutual information in chronic renal failure data, J. Biol. Syst. 15 (04) (2007) 435–451.

[24] Vijaya B. Kolachalama, et al., Association of pathological fibrosis with renal survival using deep neural networks, Kidney Int. Rep. 3 (2) (2018) 464–475.

[25] Njoud Abdullah Almansour, et al., Neural network and support vector machine for the prediction of chronic kidney disease: A comparative study, Comput. Biol. Med. 109 (2019) 101–111.

Fuzhe Ma, male, Department of nephrology, First Hospital of Jilin University, associate chief physician, doctor of clinical medicine, graduated from Bethune department of medicine of Jilin University. I have published 9 SCI papers and presided over two scientific research projects with a total scientific research fund of 150,000 yuan.

Main affiliations: member of nephrology branch of integrated traditional and western medicine society of Jilin province, member of home care association of Jilin province, member of nephrology branch of integrated traditional and western medicine society of Changchun.

Tao Sun, male, June 8, 1982, a doctor of clinical medicine, attending physician of Department of Nephrology, the First Hospital of Jilin University, graduated from the seven-year clinical medicine program of Bethune Medical College of Jilin University. He is good at diagnosis and treatment of various primary and secondary kidney diseases and acute and chronic renal failure. He is also good at grasp renal biopsy, temporary and long-term central venous catheterization, arteriovenous fistula, peritoneal dialysis catheterization and other blood purification techniques. He has participated in the National Natural Science Foundation of China and a number of provincial and ministerial research projects, and participated in the compilation of academic treatises.

Lingyun Liu, male, member of the communist party of China. I am now working in the Department of Andrology, the first hospital of Jilin University. I studied in the University of Louisville for two years as a visiting scholar. My research direction was male reproduction.

In the past five years, I have published more than 0 SCI papers, including 11 as the first author, with a cumulative impact factor of 8 points.

Hongyu Jing is a deputy chief physician doctor, graduated from Jilin University. He works at First Hospital of Jilin University Department: Respiratory Medicine. He is good at rescue and treatment of common respiratory diseases, frequently-occurring diseases and critical respiratory diseases. He has been engaged in the diagnosis and treatment of respiratory diseases for a long time. The main research direction is on the mechanism of sprouty1 protein and non-small cell lung cancer and pulmonary interstitial fibrosis. He has published 5 SCI papers as the first responsible author, with a cumulative impact factor of 14 or more, and undertook/participated in a number of provincial and ministerial projects.